Catalysis Today

Polystyrene CuO/Cu₂O uniform films inducing MB-degradation under sunlight

O. Baghriche [a,b,1], S. Rtimi [b,*,1], C. Pulgarin [b,1], J. Kiwi [b,1]

[a] Université Constantine 1, Laboratoire des Techniques Innovants de Préservation de l'Environnement (LTIPE), Constantine 25017, Algeria
[b] Ecole Polytechnique Fédérale de Lausanne, EPFL-SB-ISIC-GPAO, Station 6, CH-1015, Lausanne, Switzerland

ARTICLE INFO

ABSTRACT

This study reports on a Cu-sputtered film on polystyrene (PS) leading to the discoloration/degradation of methylene blue (MB) under low intensity solar simulated irradiation. Direct current magnetron sputtering (DCMS) was used to graft uniform, adhesive Cu/Cu oxides on the polystyrene substrate. The kinetics of Cu-PS mediated MB-discoloration adding H_2O_2 was observed to take place within 90–120 min. The surface potential and pH variation was followed on the Cu-PS surface during MB-discoloration. Insight is provided for the observed changes relating them to the dye discoloration mechanism. The concentration, mean- free path and lifetime of the oxidative radical leading to MB-degradation were estimated. The Cu/Cu-oxides on the PS were characterized by X-ray diffraction (XRD). X-ray photoelectron spectroscopy (XPS) evidence for *redox* catalysis involving Cu(I)/Cu(II)-species was detected during MB-discoloration. Also by XPS the surface atomic percentage concentration was determined for the topmost Cu-PS layers. The Cu-PS coatings were also investigated for their optical and crystallographic properties.

1. Introduction

Photocatalytic degradation of pollutants is a promising approach to face the increasing environmental contamination. Under light, photoactive titanium dioxide (TiO_2) has been shown to degrade organic compounds/dyes due to its photocatalytic properties [1,2]. However, because of its wide band gap (3.2 eV) TiO_2 can absorb only UV light ($\lambda < 387$ nm), about 4–5% of the whole solar spectrum. Sensitization of the TiO_2 by doping with Cu/CuO has been shown to be attractive approach to extend the TiO_2 response into the visible region [3,4]. This approach is used in this study to improve the TiO_2 reaction kinetics under the visible light irradiation during discoloration of the probe dye methylene blue (MB).

The use of photocatalysts in the form of colloids, powders and flakes is costly since it has to be separated after the cleaning process. Therefore, TiO_2 deposited on various substrates like glass and thin polymer films have been investigated for over three decades mainly being activated by UV-light to avoid the time, cost and materials involved in the separation step. TiO_2 colloids have been deposited on supports by calcination on heat resistant substrate supports. On low heat resistant surfaces/polymers, the support will no withstand precluding TiO_2 annealing to attain good adhesion. Colloids annealed at lower temperatures do not withstand friction, are easily wiped out, and are not reproducible or mechanically resistant [5]. To avoid the problems inherent to colloidal particle deposition on low thermal resistant substrates, this study focuses on the sputtering of Cu/Cu₂O/CuO films on PS. The interest of using polystyrene (PS) resides in the fact that it is a low cost, inert, no-toxic widely available thermoplastic polymer.

During the last few years there has been a growing interest in the preparation of PS films as a substrate for TiO_2 nanoparticles in the area of photocatalytic degradation of organic compounds. The interest to degrade the MB dye resides in the fact that MB- is widely used in printing/dyeing industries inducing eye irritation, vomiting and cyanosis [6]. Yang et al., [7] reported TiO_2 anchored on PS degrading MB under UV-light within 3–4 h. TiO_2 Degussa P25 PS was dip-coated on PS by Singh et al., [8] and led to partial MB-degradation within a few hours.

To extend the TiO_2 absorption into the visible range, several laboratories have recently reported TiO_2-F and TiO_2-N doped PS films prepared by colloidal methods degrading organic compounds under sunlight light within a few hours J. K. Zhou et al., report degradation of MB [9], K. M. Parida et al., report degradation of methyl-orange (MO) and MB, an anionic and a cationic dye [10]. V. Viano et al., report the degradation of MB [11], L. Huang et al., [12] reports MO degradation and Z. Zheng et al., [13] et al., have reported Cu(I)O and Cu(II)O active in the photocatalytic degradation of pollutants/dyes under visible light up to 680 nm.

The fact that CuO and Cu_2O absorb light in the range of the solar radiation with a band-gap < 2 eV and is a low cost oxide has led to the its use in environmental processes [14–16]. Recently, ppb amounts of Cu were sputtered on TiO_2 or TiO_2-ZrO_2 giving rise to materials with improved self-cleaning applications by way of the Cu intra-gap states in the TiO_2 matrix [16,17]. The nature of these intra-gap states in TiO_2 is far from been understood at the present time and more work is needed in this direction [18].

The novelty presented in this work is the grafting of Cu/CuO uniform, adhesive and stable thin films on polystyrene (PS) leading to a MB-degradation in acceptable times under low intensity sunlight. The times of MB-degradation found in the present study were shorter than the times reported until now irradiated by UV-light. This implies a reduction in the use of electrical energy. Optimization of the sputtered film thickness to attain the most suitable MB-degradation times was carried out during the course of this study. The characterization of the Cu/CuO PS film properties is also reported in the present work.

2. Experimental

2.1. Materials, irradiation procedures, Cu-sputtering and Cu-thickness calibration, DRS of Cu-films and determination of MB-discoloration

The MB and H_2O_2 were Merck reagents (Buchs, Switzerland) and used as received. NaN_3 Fluka was used as singlet oxygen scavenger ($^1O_2$). 1,4-benzoquinone (BQ) and methanol were used respectively as $O_2^{\bullet-}$ radical and HO·-scavengers. Ethylenediamine tetra-acetic acid (EDTA-2Na) was used as CuO_xvb hole scavenger. To complex the Cu-species leached out from the sputtered Cu/CuOx-film, batho-cuproin disulfonate (4 μM) and sodium ascorbate (10 μM) were added to the MB-solution before contacting the Cu-sputtered polystyrene. This ascorbate concentration is added to minimize the batho-cuproin disulfonate fluorescence quenching due to the reductant (Cu/CuO). Under these conditions, the copper on the PS-film is reduced to Cu(I) and chelated by batho-cuproin disulfonate.

The Cu sputtered PS-Petri-dishes were placed into the cavity of Suntest solar simulator (Atlas, Heraeus, Germany) cavity tuned at 50 mW/cm^2, one half of the maximum solar light intensity. This experimental set-up is shown in Fig. 1a. Thin Cu films were sputtered on PS by direct current magnetron sputtering (DCMS) at 100 mA–300 mA and ~400 V in Ar atmosphere at a working pressure of ~0.1 Pa using a 2 inches Cu-target obtained from K. Lesker, Hastings, UK. The Petri dish was positioned perpendicular to the Cu-target at a distance of 10 cm. Cu-sputtering was on Si-wafers was carried out by profilometry to determine the Cu thickness deposited on PS as a function of sputtering time (Alphastep500, TENCOR). The UV–vis spectra during MB-discoloration were followed at the MB 664 nm peak in a Schimadzu single beam instrument. The Indole concentration was also followed spectrophotochemically at 270 nm due to the relatively large molar absorption coefficient of Indole of 3.2×10^3 $M^{-1}cm^{-1}$. Diffuse reflectance spectroscopy (DRS) of Cu sputtered films was
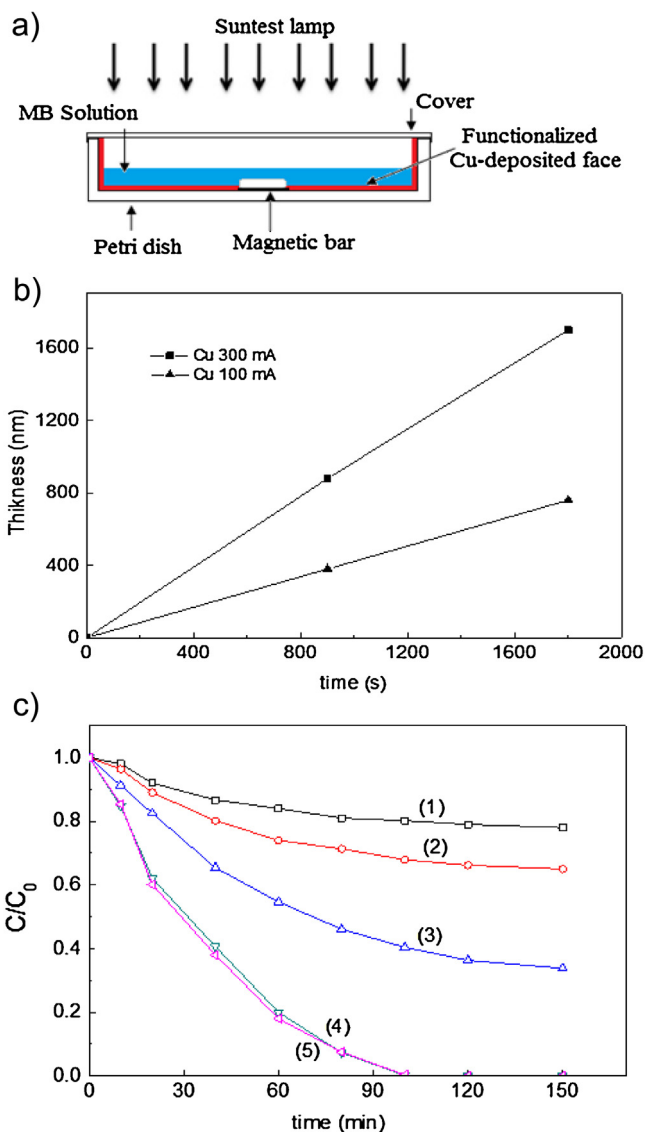
Fig. 1. a Petri-dish micro-reactor used for MB irradiation. **b.** Thickness calibration of Cu layers on Si-wafers at two different sputtering energies. **c.** Effect of the Cu-polystyrene films sputtered for 1) 5s, 2) 10s, 3) 20s, 4) 40 s and 5) 50 s on the MB discoloration kinetics of a solution containing MB(10 mg/l) and H_2O_2 (5 mM).

carried out a Perkin Elmer Lambda 900 UV-VIS-NIR spectrometer within the wavelength range of 200–800 nm.

2.2. TOC determination, released cu as determined by ICP-MS, pH/surface potential changes on Cu-PS and oxidative radicals within MB-discoloration

The total organic carbon (TOC) was determined in a Shimadzu TOC-500 instrument equipped with an ASI auto-sampler. De-ionized water 18MΩcm and with a content of dissolved organic carbon (DOC) < 0.1 mg C/L obtained by using a Millipore (Milli-Q) water. The determination by inductively coupled-plasma mass-spectrometry (ICP-MS) of the Cu released during MB-degradation was carried out in a Finnigan inductively coupled-plasma mass-spectrometer.

The redox potential and pH were during the MB discoloration were followed using the nano-volt/micro-Ohm meter with platinum electrodes and the surface-pH in the Petri-dish micro-reactor were recorded using a high-precision pH meter (Jenco Electronics 6230N, San Diego, USA). The device was monitored via RS-232-C

IBM compatible communication interface and BNC, pH/ORP connector with 8-pin DIN ATC connector. The pH meter was able to record the pH-changes in the seconds scale with a high degree of pH sensitivity of 0.01 pH units. The electrode was immersed in the micro-reactor and the measurements were taken after a suitable delay required for the sample stabilization.

2.3. X-ray diffraction and XPS of Cu-PS

The crystalline structure of the Cu/CuOx-PS films was investigated by X-ray diffraction (XRD) and recorded on an X'Pert MPD PRO from PANalytical equipped with a secondary graphite (002) monochromator and an X'Celerator detector operated in Bragg–Brentano geometry. The X-ray photoelectron spectroscopy (XPS) of the Cu/CuOx-PS was measured using an AXIS NOVA photoelectron spectrometer (Kratos Analytical, Manchester, UK) provided for with monochromatic AlK$_a$ (hν = 1486.6 eV) anode. The carbon C1s line with position at 284.6 eV was used as a reference to correct for the charging effects. The surface atomic concentration was determined from peak areas using the known sensitivity factors for each element [19,20]. Spectrum background was subtracted according to Shirley [21] and the XPS spectral peaks were deconvoluted with a CasaXPS-Vision 2, Kratos Analytical UK.

3. Results and discussion

3.1. Effect of the Cu-film thickness and effect of added H_2O_2 on the MB-discoloration kinetics and photocatalyst recycling

Fig. 1b indicates for Cu-sputtered at 300 mA a thickness of 100 nm after 100s. Therefore, 1 nm was sputtered within 1s, this is equivalent to about 5 Cu-atomic-layers each one of 0.2 nm. Taking a 0.3 nm lattice distance between the Cu-atoms, about 10^{15} Cu-atoms can be estimated per cm^2. The Cu-deposition proceeds with 5×10^{15} atoms/cm^{2}xs. Fig. 1b shows in the thickness calibration a $\pm$10% experimental error. Fig. 1c shows the discoloration kinetics of MB under low intensity solar light on Cu-PS. It is readily seen that the fastest discoloration is attained on Cu-sputtering for 40 s on films with a thickness of ~35 nm (~175 atomic layers). At a sputtering time of 40s, the thickness of the Cu/Cu-oxide film allows the Cu-nanoparticulate to present the highest amount of Cu-sites held in exposed positions interacting with the polystyrene substrate.

Fig. 2a shows the effect of the H_2O_2 concentration on the MB-discoloration. Fig. 2 shows the MB-discoloration kinetics upon addition of H_2O_2 (5 mM) and H_2O_2 (1 mM). Next Fig. 2a, traces 3 and 4) showa that in the absence of Cu, the oxidation slows down drastically. If higher H_2O_2 concentrations > 10 mM were added, the MB discoloration kinetics were seen to slow down due to the known scavenging of the OH$^\circ$-radical in the solution as shown in eq (1)

$$H_2O_2 + HO^\cdot \rightarrow H_2O + HO_2^\circ \; 3.0 \times 10^7 \, M^{-1}s^{-1} [22, 23] \qquad (1)$$
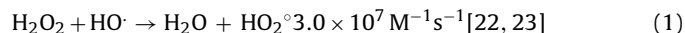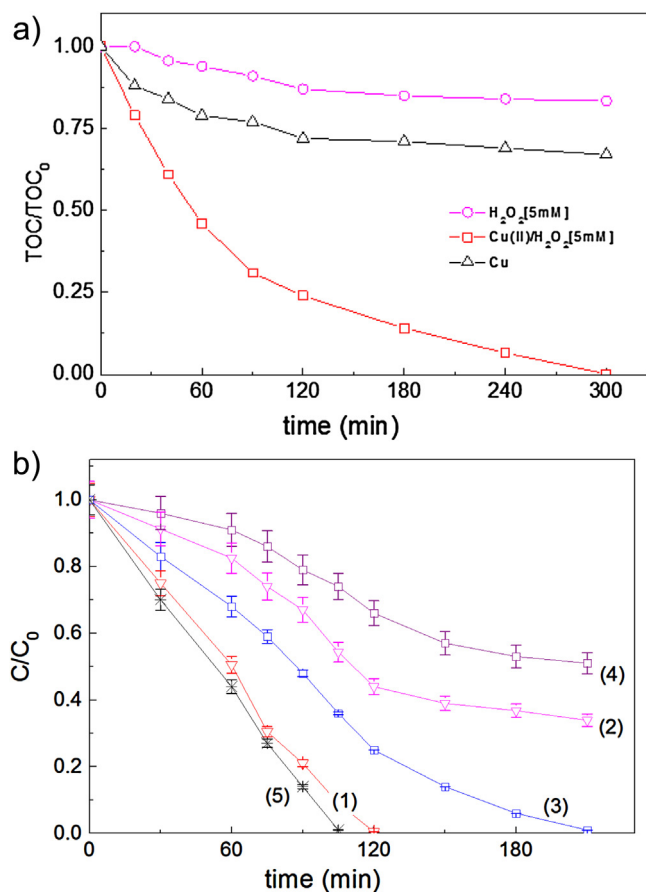
and this explains the low k value in Fig. 2b upon addition of 20 mM H_2O_2. During MB degradation the initial pH of 5.4 decreases to 4.2 after 90 min. Therefore in eq (1) the HO$_2$$^\circ$ and not O$_2$$^-$ would be the predominating species in solution. Fig. 2c shows the repetitive MB discoloration up to the 5th cycle. After each discoloration the Cu-PS film was thoroughly washed with tri-distilled water before reuse.

By inductively coupled plasma coupled mass-spectrometry (ICP-MS) the Cu-ions release during the first MB-discoloration was determined for Cu-PS samples sputtered for 40 s in the presence of H_2O_2 (5 mM). For the run shown in Fig. 2a, trace 1) about 5 ppb (μg/L) were found after 120 min. For the runs reported in Fig. 2c, the Cu-ion release was observed to reach 9 μg/l $\pm$ 15% after the 5th cycle. The small amount of Cu-ions released in the ppb
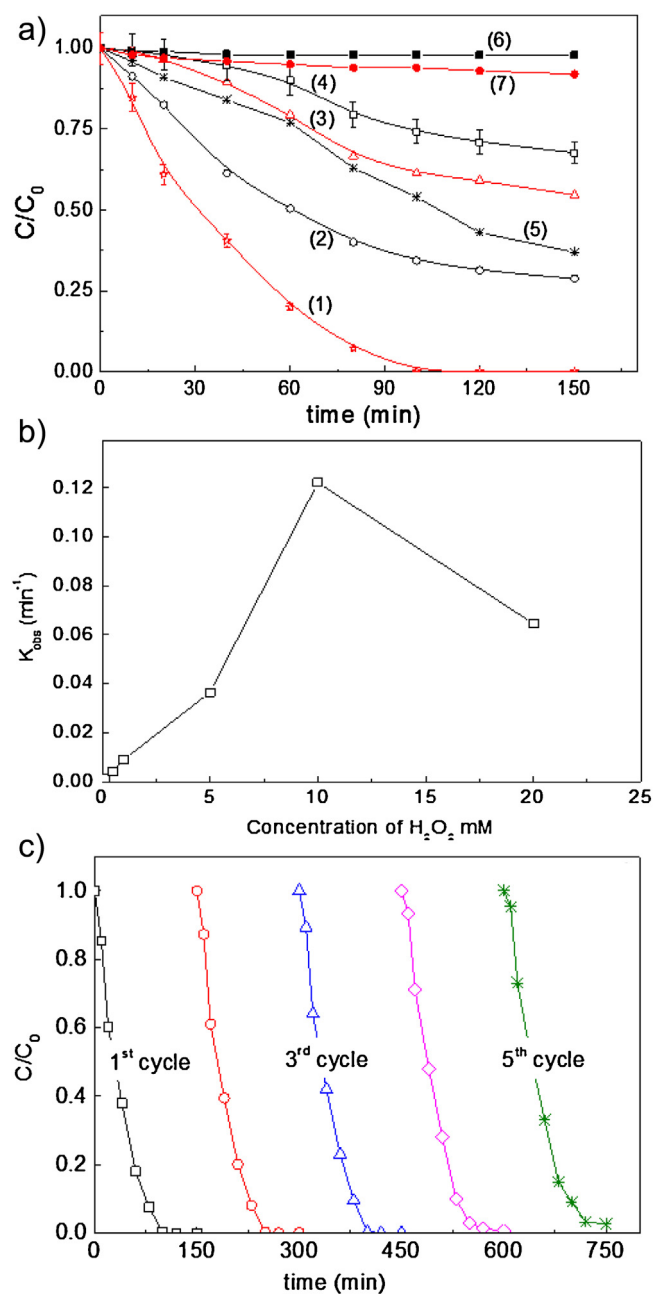
Fig. 2. a Degradation of MB (10 mg/l) under low intensity solar simulated light. irradiation (50 mW/cm^2) on 1) Cu-polystyrene sputtered for 40s + H_2O_2 (5 mM); 2) Cu-polystyrene sputtered for 40s + H_2O_2 (1 mM); 3) only H_2O_2 (5 mM) in uncoated PS Petri dish; 4) H_2O_2 (1 mM) in uncoated PS Petri dish; 5) Cu-PS Petri-dish micro-reactor 6) Cu-PS Petri-dish micro-reactor in the dark 7) PS Petri-dish micro-reactor in the dark. b Effect of the initial concentration of H_2O_2 on the MB (10 mg/l) discoloration kinetics in the presence of Cu-PS Petri-dish micro-reactor sputtered for 40 s under 50 mW/cm^2 solar simulated light. c Repetitive photo-degradation of MB (10 mg/l), initial pH 5.4 in Cu-PS (Petri-dish) sputtered for 40 s + H_2O_2 (5 mM) under low intensity solar simulated light (50 mW/cm^2).

range during MB-discoloration excludes any Fenton-like type reactions in solution. Fenton type reactions require generally above 2 mg/l. This is ~400 times the amount Cu-released during the repetitive MB-discoloration shown in Fig. 2c (μg/L). The concentration of H_2O_2 added in solution is shown in Fig. 2b. By the data shown in Fig. 2b, and by inspection of eq (1) the added concentration of H_2O_2 is seen the most important factor limiting the MB discoloration/degradation kinetics. To treat higher volumes of MB-solutions it is important to proceed with an acceptable kinetics
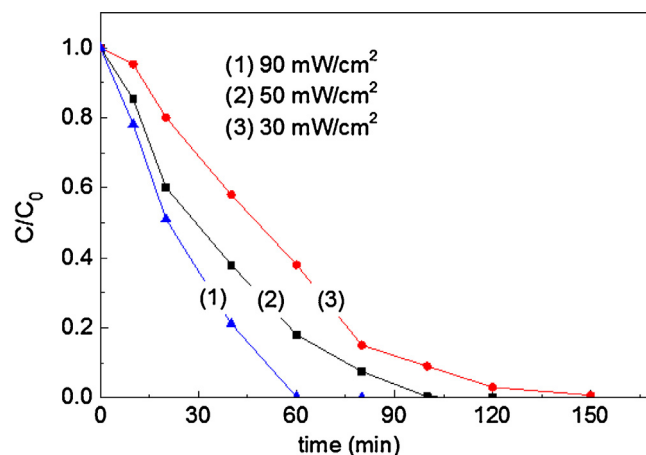
Fig. 4. Effect of the applied solar simulated light intensity on the discoloration of MB (10 mg/l) in Cu-PS sputtered for 40 s + H_2O_2 (5 mM).
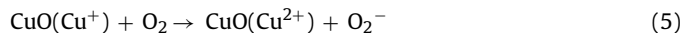
sputtered for 40 s increased only marginally the Indole degradation kinetics compared to the data shown for the Indole degradation in its absence (Fig. 3b, trace 1) suggesting the predominant role of O_2 in the photodegradation.

3.2. Effect of the light intensity on the MB-discoloration, semiconductor behavior leading to the generation of charges on the Cu-PS surface

Fig. 4 shows the effect the light intensity on the MB-discoloration kinetics. The MB-discoloration kinetics on the applied light intensity provides the evidence for the Cu-PS acting through a CuOx associated semiconductor behavior comprising the photo-generation of charges under band-gap irradiation [1–4]. Fig. 4 shows that the MB-discoloration kinetics becomes longer when a lower number of photo-generated charge carriers are induced by a lower light intensity. The CuO under sunlight irradiation photo-generates charges

$$CuO + h\nu(sunlight) \rightarrow CuO(cbe\text{-}), CuO(vbh+) \qquad (2)$$
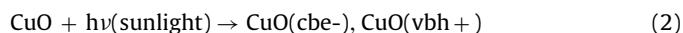
Under photon energies exceeding the CuO band-gap, the cbe-electron could either react directly with the O_2 forming O_2^- eq(3) or reduce the Cu^{2+} to Cu^+ as noted in eqs.(3–5):

$$CuO(cbe\text{-}) + O_2 \rightarrow CuO + O_2^- \qquad (3)$$

$$CuO(cbe\text{-}) \rightarrow CuO(Cu^+) \qquad (4)$$

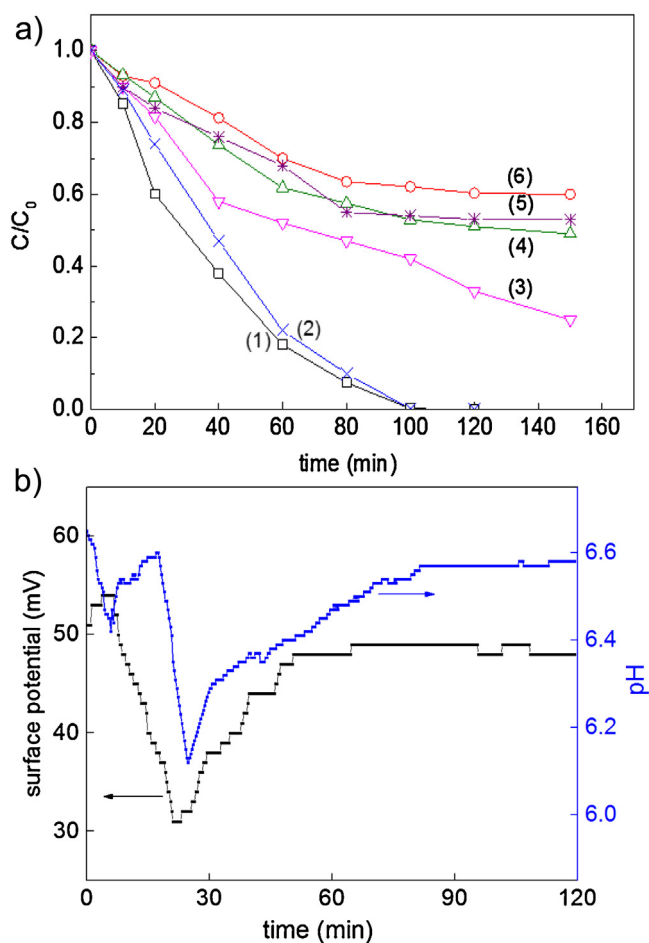$$CuO(Cu^+) + O_2 \rightarrow CuO(Cu^{2+}) + O_2^- \qquad (5)$$

The cbe- in eq(2) is produced by a CuO (*p*-type) with band-gap energy of 1.7 eV, a flat-band potential of −0.3 V SCE (pH 7), and a valence band at +1.4 V SCE [14].

$$CuO(Cu^+) \rightarrow CuOvacancy + Cu^+ \qquad (6)$$
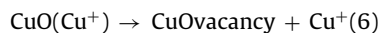
3.3. Quenching of oxidative radicals during MB-degradation on Cu-PS: changes in the surface pH and e potential during MB-degradation

The data in Fig. 5a suggests only the presence of oxidative radicals in the solution [25]. By the use of the commonly radical scavengers [1,2], the data in by adding azide (NaN_3) suggests the possible presence of singlet oxygen (trace 3). Benzoquinone and EDTA-2Na have been reported as scavengers of HO_2· (trace 4) and CuOvb(+) (trace 5). Methanol has been widely reported as an HO·-scavenger (trace 6). Azide has been reported as a singlet

Fig. 3. a Mineralization of a solution MB (10 mg/l, at initial pH 5.4) under low intensity solar simulated light (50 mW/cm²) the presence of 1) Cu-PS sputtered for 40 s + H_2O_2 (5 mM) 2) only Cu-PS Petri-dish micro-reactor and 3) only H_2O_2 (5 mM) on unsputtered PS. b Indole degradation on Cu-PS: (1) Cu-PS sputtered for 40 s degrading 10 mg/l Indole, (2) Cu-PS sputtered for 40 s degrading 20 mg/l Indole, (3) Cu-PS sputtered for 20 s degrading 10 ppm Indole, (4) Cu-PS sputtered for 20 s degrading 20 mg/l Indole and (5) Cu-PS sputtered for 40 s degrading 10 mg/l Indole in the presence of H_2O_2 (5 mM). Intensity: 50 mW/cm² solar simulated light.

before for any practical application. We have set the initial MB-concentration at 10 mg/l. But higher MB-concentrations would also limit the kinetics of MB-abatement. Therefore, suitable dilutions of MB should be selected to attain an acceptable kinetics during MB-degradation.

The mineralization of MB is shown in Fig. 3a. In the presence of Cu-PS/H_2O_2, the MB-mineralization was completed within 5 h, a time longer compared to the MB discoloration time. The control runs in Fig. 3a shows that MB-mineralization was not complete under the same conditions used in the presence of the photocatalyst.

To address the question if the CuOx cb-electrons will transfer to a colorless pollutant and photo-activate its photo-degradation, Indole was selected as the probe. Indole absorbs <294 nm [1,2]. Fig. 3b shows the effective degradation of Indole when CuOx was the only light absorber of the incoming radiation. Within ~100 min, the Cu-PS sputtered for 40 s induced Indole degradation as seen in Fig. 3b, trace 1). At a higher Indole concentration Fig. 3b, trace 2) shows degradation of Indole slowing down as expected. A lower amount of CuOx shows in Fig. 3b, trace 3) indices indole degradation but in ~200 min. In this case the amount of CuOx in the Cu-PS surface is lower compared to the one found in Cu-PS sputtered for 40 s (Fig. 3b, trace 1). An increase in the Indole concentration using the Cu-PS sputtered for 20 s leads to a slower degradation as reported in Fig. 3b, trace 4). Finally, the addition of H_2O_2 (5 mM) to CU-PS

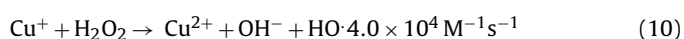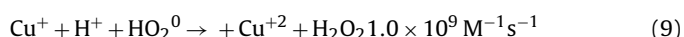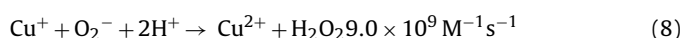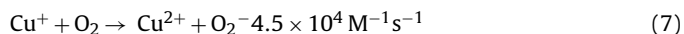**Fig. 5.** a Discoloration of a solution MB (10 mg/l) irradiated by solar simulated light (50 mW/cm^2) on Cu-PS sputtered for 40s + H$_2$O$_2$ (5 mM). Runs: (1) no scavengers added, (2) addition of bathocuproin disulfonate, (3) addition of NaN$_3$ (0.2 mM), (4) addition of benzoquinone (0.2 mM), (5) addition of EDTA-2Na (0.2 mM) and (6) addition of methanol (0.2 mM). For other details see text. b Surface pH-changes and changes in the surface potential on Cu-PS films during the MB-degradation (10 mg/l) under solar simulated light (50 mW/cm^2).

oxygen scavenger. But it also reacts with HO·-radicals with a similar rate similar as it does with singlet oxygen [25]. Therefore, the data in Fig. 5a does not unambiguously prove the generation of singlet oxygen. The batho-cuproin added, a complexing agent for the Cu(II)/Cu(I)-ions (see Experimental Section) did not inhibit the MB-discoloration kinetics. This suggests that reaction (5) involving CuO(Cu$^+$) and possibly the reaction of the CuO with the holes vb(h+) is much faster than the CuO dissolution shown in reaction (6). EDTA is considered as a hole-scavenger in the case of TiO$_2$ photocatalysis. But it may not play this role in the case of copper oxide materials [25].

The Cu$^+$/Cu^{2+} ions detected by ICP-MS may lead to MB-degradation through reactions 7–12 in the presence of H$_2$O$_2$ [23,24,26–28].

$$Cu^+ + O_2 \rightarrow Cu^{2+} + O_2^- \quad 4.5 \times 10^4 \, M^{-1}s^{-1} \tag{7}$$

$$Cu^+ + O_2^- + 2H^+ \rightarrow Cu^{2+} + H_2O_2 \quad 9.0 \times 10^9 \, M^{-1}s^{-1} \tag{8}$$

$$Cu^+ + H^+ + HO_2^0 \rightarrow \, + Cu^{+2} + H_2O_2 \quad 1.0 \times 10^9 \, M^{-1}s^{-1} \tag{9}$$

$$Cu^+ + H_2O_2 \rightarrow Cu^{2+} + OH^- + HO· \quad 4.0 \times 10^4 \, M^{-1}s^{-1} \tag{10}$$

$$Cu^{2+} + O_2^- \rightarrow Cu^+ + O_2 \quad 4.5 \times 10^4 \, M^{-1}s^{-1} \tag{11}$$

$$Cu^{2+} + HO_2^0 \rightarrow Cu^+ + O_2 + H^+ \quad 5.0 \times 10^7 \, M^{-1}s^{-1} \tag{12}$$
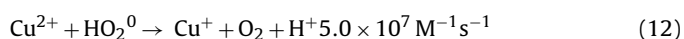
The changes in pH and surface potential were followed within the time of bacterial inactivation and the results are presented next in Fig. 5b. This approach allows some insight into the changes on the surface of the film during MB-degradation Fig. 5b presents the surface pH-shift at the Cu-PS interface under low intensity solar light irradiation. A pH-decrease between 6.7 and 6.1 was observed within 25 min. The decrease in pH-shift is equivalent to a six-fold increase in the concentrations of [H$^+$]. The pH decrease is due to short chain carboxylic acids generated in solution during MB-degradation. These carboxylic acids have pi$_{ke}$ values around ~3 [27,28]. After ~30 min, the pH recovers up to ~6.6 due to the CO$_2$ generation by the short carboxylic. This is the final step in MB-degradation. This step is known as the photo-Kolbe CO$_2$ reaction [29] and is shown below in eq(13):

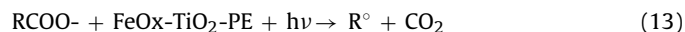$$RCOO\text{-} + FeOx\text{-}TiO_2\text{-}PE + h\nu \rightarrow R^\circ + CO_2 \tag{13}$$

Fig. 5b shows also that the interface potential decrease of Cu-PS decreases from 60 to ~30 mV within 30 min. The voltage decrease is due to changes in the surface microstructure during the initial stage of MB-discoloration. The surface potential recovery after 30 min up to 55 mV and reflects the recovery of the initial Cu-PS surface structure after the initial MB-degradation.

3.4. Estimation of the concentration, mean-free path and lifetime of the HO·-radical during MB-degradation and leuco-MB form considerations

In a dilute MB-solution with a make-up: MB = 3 × 10^{-5} M, H$_2$O$_2$ = 5 × 10^{-3} M and the concentration of the Cu released into the solution of 5 ppb ≅ Cu ~10^{-7} M (see Section 3.1) allows the estimation of the OH·-concentration in solution taking into account the reactions

$$Cu + H_2O_2 \rightarrow Cu^+ + OH^- + HO· \quad k_1 = 4 \times 10^5 \, M^{-1}s^{-1} [24] \tag{14}$$
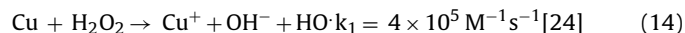
and b) the rate of the reaction of OH· with an aromatic compound in eq.(15):

$$HO· + MB(RH) \rightarrow products \quad k_2 \sim 10^{10} \, M^{-1}s^{-1} [1, 2] \tag{15}$$
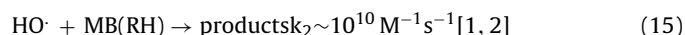
$$\frac{dHO^\circ}{dt} = k_1[Cu][H_2O_2] - k_2[OH·][MB] \cong 0 \tag{16}$$

Assuming the quasi-stationary state for the HO·-radical concentration close to zero, it is possible to estimate by way of eq (15) a value of ~6 × 10^{-10} M for the HO·-radical concentration (see for details Supplementary material S1).

The leuco form of MB (LMB$^-$) is colorless in absence of O$_2$, but rapidly oxidizes to blue cationic MB$^+$ in air and in the presence of Cu-ions. In the present study we have detected <10 μg/l of Cu present in solution. This is much lower than the Cu concentration of 10^{-4} M necessary to catalyze the re-oxidation of LMB- to MB$^+$ since this Cu-catalyzed re-oxidation has been reported at Cu concentrations > 10^{-4}M in acid media [30,31]. The re-oxidation of the MBL- has been reported to be a function of a) the amount of O$_2$ dissolved in the aqueous solution and b) the solution pH [32,33].

The Smoluchowski simplified approximation x^2 = Dτ is used next to estimate the OH·-radical mean-free path (x) away from the Cu-PS surface. Being D the diffusion of molecules with a low molecular weight species like MB of 5 × 10^{-6} cm^2/s and 1/τ the inverse of the encounter pair lifetime τ = 1/(k$_{OH}$ + MB) x [MB] of 3.3 × 10^{-6} s and inserting this last value in the relation x^2 ~ Dτ, the mean-free path was found to be x ~40 nm.

Finally, the lifetime of the HO·-radical could be estimated by the product of the inverse of the H$_2$O$_2$ concentration (5 mM) time k$_3$ the reaction rate between the HO· and H$_2$O$_2$ [1,2]. For additional explanations see Supplementary material S1.
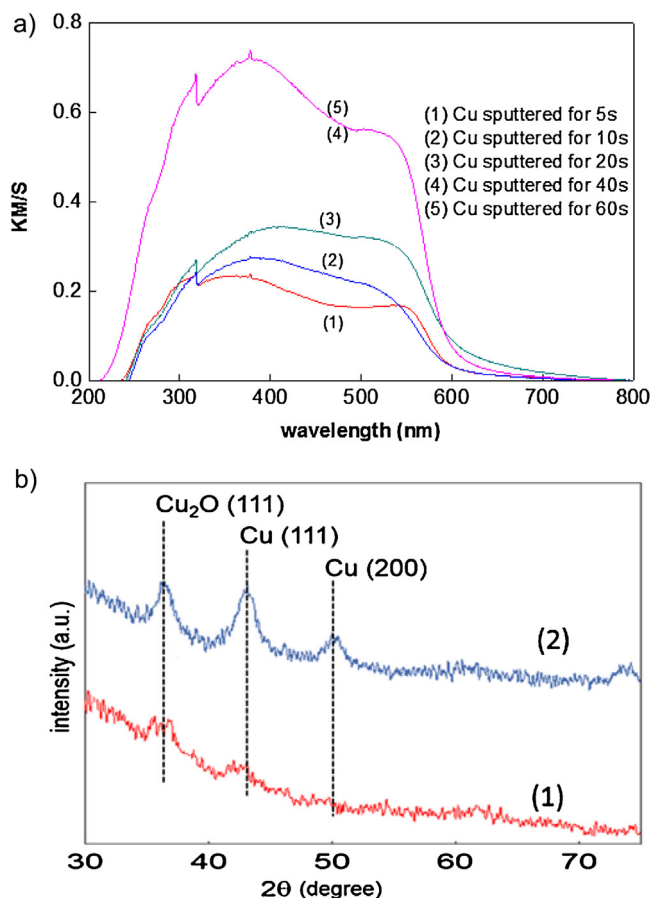
Fig. 6. a Diffuse reflectance spectroscopy (DRS) of the Cu-PS sputtered for times: (1) 5 s (2) 10 s (3) 20 s (4) 40 s and (5) 60s. b X-ray diffraction (XRD) spectrograms for 1) Cu-PS sputtered at 100 mA and 2) and 300 mA.

3.5. Characterization of the Cu-polystyrene films by diffuse reflectance spectroscopy (DRS), X-ray diffraction (XRD) and X-ray photoelectron spectroscopy (XPS)

The diffuse reflectance spectra (DRS) in Fig. 6a show an increase in the optical absorption in Kubelka-Munk units as a function of the Cu sputtering time up to 60s. The rough UV–vis reflectance data cannot be used directly when accounting for the absorption coefficient of the Cu/CuOx-PS due to the large scattering contribution to the reflectance spectra of the film. Normally a weak dependence is assumed for the scattering coefficient S on the wavelength. The Petri-dish PS was coated on the bottom and the surrounding walls. The Petri-dishes walls reflect the incoming light further increasing the light absorption by the photocatalyst. The optical absorption in Fig. 6a was observed between 200 and 720 nm [34]. The optical absorption in the region between 500 and 600 nm is due to the inter-band transition of Cu(I) between 600 and 700 nm has been assigned to the Cu(II) d–d transition [35].

Fig. 6b presents the X-ray diffraction of Cu-PS sputtered for 40 s at 100 and 300 mA. Fig. 6b does not show sharp peaks for the Cu/CuO clusters, since the Cu-clusters are not fully crystallized. This may be due to: a) the small size of the Cu-nanoparticles clusters on the PS due to the short sputtering time and/or b) the low Cu-loading attained after sputtering for 40 s (~175 layers). The Miller (h, k, l) index for the three peaks in Fig. 6b corresponds to a) the face centered cubic crystal (FCC), b) the Cu_2O (111) and c) the Cu (111) peaks. The noise to signal ratio in Fig. 6b was due to the low amount of Cu-species sputtered on the substrate.
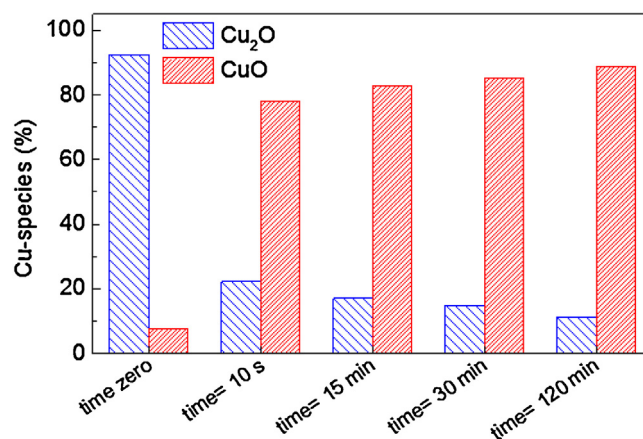
Fig. 7. Variation in the Cu_2O and CuO-percentages detected by XPS on Cu-PS up to 120 min during the MB-discoloration in a solution MB (10 mg/L) in the presence of H_2O_2 (5 mM) under solar simulated light (50 mW/cm^2).

Table 1
Surface atomic percentage concentrations of elements on Cu-polystyrene (Cu-PS) during MB-discoloration under low intensity solar simulated light.

	C1s	Cu2p	O1s	N1s
Time zero	6.35	65.24	28.41	–
Contacted with MB for 10 s then washed	43.66	28.11	22.21	6.03
After MB discoloration (120 min)	30.17	43.24	23.96	2.63

Fig. 7 presents the XPS of the Cu-oxidation states before and after MB-discoloration. At time zero the Cu-film in Fig. 7 shows that freshly sputtered Cu-films consists of Cu_2O that within 10 s is oxidizes to CuO. The percentage of Cu_2O decreases from 92% to 12% up to 120 min and the CuO increased from 5% to 90%. The CuO 2p3/2 peak was followed at 934.3 eV and the peak of Cu_2O 2p3/2 at 932.1 eV to report the information presented in Fig. 7 [19–21]. The progressive shifts in the Cu_2O 2p3/2 peaks to CuO 2p3/2 peak from 934.31 eV to 934.1 eV provides the evidence for the *redox* catalysis during MB-discoloration[19].

The surface atomic concentration percentage changes during the MB-degradation are presented in Table 1. The C1 s peak at time zero on the Cu-PS shows a low value for C- suggesting that most of the PS was covered by the sputtered Cu-layers. After contacting Cu-PS with the MB solution for 10 s the higher C-content is due to the added MB. The C1 s percentage decreases afterwards due to the MB-degradation up to 120 min. The Cu 2p3/2 signal is high on the Cu-PS film at time zero decreasing upon contact with MB and increases again after 120 min when the residues due to the MB-degradation are removed from the Cu-PS surface. This observation is consistent with the TOC decrease reported during MB-degradation in Fig. 3. Finally, no N 1s peak signal was recorded at time zero, but appeared after contact with MB due to N- in the MB structure. As expected the N-content was seen to decrease after 120 min the time of MB-degradation.

4. Conclusions

This study presents the preparation of an innovative uniform, stable and adhesive sputtered Cu-PS photocatalyst at low temperature by DC-magnetron sputtering. This is the first report on uniform coatings of Cu/CuO on PS catalysts leading to the degradation of a model dye. The MB-discoloration kinetics in the presence of H_2O_2 was completed within 90–120 min. The degradation of MB occurs within a time about 3 times shorter than its mineralization, suggesting the formation of long-lived intermediates during MB-mineralization. During the degradation of MB, CuO intervenes as a

semiconductor since the MB degradation kinetics was observed to be a function of the applied light intensity. The Cu-PS films released Cu in ppb amounts during repetitive MB-discoloration cycles showing the stability and the potential for their long-term operational use. The surface properties of the Cu-PS films were investigated by several surface science methods reporting the film optical absorption, the Cu_2O and CuO crystallography by XRD and the surface atomic percentage concentration by XPS measurements. Evidence was also presented for the occurrence of *redox* catalysis involving Cu(I)/Cu(II) on PS by XPS during MB degradation.

Acknowledgments

Appendix A. Supplementary data

Supplementary data associated with this article can be found, in the online version, at http://dx.doi.org/10.1016/j.cattod.2016.10.018.

References

[1] A. Fujishima, X. Zhang, D. Tryk, 63 (2008) 515–546.
[2] J. Schneider, M. Matsuoka, M. Takeuchi, J. Zhang, Y. Horiuchi, M. Anpo, D. Bahnemann, Chem. Rev. 118 (2014) 9919–9986.
[3] S. Banerjee, D. Dionysiou, S.C. Pillai, Appl. Catal. B 176–177 (2015) 396–428.
[4] M. Pelaez, N. Nolan, S.C. Pillai, M. Seery, Po Falaras, A. Kontos, M.S.P. Dunlop, J. Hamilton, J.-A. Byrne, K. O'Shea, M. Entezari, D. Dionysiou, Appl. Caalt. B 125 (2012) 331–345.
[5] L. Zhang, R. Dillert, D. Bahneman, M. Vormoor, Energy Environ. Sci. 5 (2012) 7491–7499.
[6] S. Sing, H. Mahalingan, P.K. Singh, Appl. Catal. A 462–463 (2013) 178–195.
[7] J.-H. Yang, Y.-S. Han, J.-H. Choy, Thin Solid Films 495 (2006) 266–271.
[8] S. Singh, A. Chaki, D.P. Chand, A. Raghuwanshi, P.K. Singh, J. Chem. Eng. 28 (2014) 9–13.
[9] J.K. Zhou, L. Liv, J. Yu, H.L. Li, P. Guo, H. Sun, X.S. Zhao, J. Phys. Chem. C 112 (2008) 5316–5321.
[10] K.M. Parida, B. Naik, J. Colloid Interf. Sci. 333 (2009) 269–276.
[11] V. Viano, O. Sacco, D. Sannino, G. Guerra, J. Chem. Technol. Biotechnol 89 (2014) 1175–1181.
[12] L. Huang, F. Peng, H. Yu, H. Wang, Solid State Sci 11 (2009) 129–138.
[13] Z. Zheng, B. Huang, Z. Wang, M. Guo, X. Qin, X. Zhang, P. Wang, Y. Dai, J. Phys. Chem. C 113 (2009) 14448–14453.
[14] A. Nozik, Ann. Rev. Phys. Chem. 189 (1978) 521–549.
[15] E. Kusiak-Nejman, A.W. Morawski, A.P. Ehiasarian, O. Baghriche, C. Pulgarin, E. Mielczarski, J. Mielczarski, A. Kulik, J. Kiwi, J. Phys. Chem. C 115 (2011) 21113–21119.
[16] S. Rtimi, O. Baghriche, C. Pulgarin, J.-C. Lavanchy, J. Kiwi, Surf. Coat. Technol. 232 (2013) 804–813.
[17] S. Rtimi, C. Pulgarin, R. Sanjines, J. Kiwi, Appl. Catal. B 180 (2016) 648–655.
[18] R. Fagan, D.E. McCormack, D. Dionysiou, S.C. Pillai, Mater. Sci. Semiconductor Process. 43 (2016) 2–14.
[19] Handbook of X-ray Photoelectron Spectroscopy C. D. Wanger, W. M. Riggs, L. E. Davis, J. F. Moulder and G. E.Muilenberg Perkin-Elmer Corp., Physical Electronics Division, Eden Prairie, Minnesota, USA, 1979. p.190.
[20] J. Nogier, M. Delamar, P. Ruiz, P. Albers, J. Kiwi, XPS and SIMS characterization, Catal. Today 56 (2000) 403–413.
[21] D.A. Shirley, High-resolution X-ray photoemission spectrum of the valence bands of gold, Phys. Revs. B 5 (1972) (1972) 4709–4714.
[22] M.D. Stanbury, Adv. Inorg. Chem. 33 (1989) 69–76.
[23] P. Wardman, J. Phys. Chem. Ref. Data 18 (1989) 1637–15755.
[24] E. Lipczynska-Kochany, Chem. Oxidation 3 (1994) 12–27.
[25] A. Mills, personal communication 2016.
[26] E. Lipczynska-Kochany, J.R. Bolton, Env. Sci. Technol. 26 (1992) 259–261.
[27] L.M. Dorfman, G.E. Adams, Report No NDRDS-NBS-46, US Government, Washington, D.C, 1973.
[28] G.V. Buxton, C.L. Greenstock, W. Ph Helman, A.B. Ross, J. Phys. Chem. Ref. Data 17 (1988) 513–589.
[29] A. Kraeutler, A. Bard, J. Am. Chem. Soc. 1100 (1978) 239–2244.
[30] O. Impert, A. Katafias, P. Kita, A. Mills, A. Pietkiewicz-Graczyk, G. Wrezeszcz, Dalton Trans. (2003) 348–353.
[31] S. Lee, A. Mills, Chem. Com. 236 (2003) 6–2367.
[32] A. Mills, J. Wang, J. Photochem. Photobiol. A 127 (1999) 123–134.
[33] J. Zita, A. Krysa, A. Mills, J. Photochem. Photobiol. A 127 (1999) 123–134.
[34] K. Hardee, J. Bard, J. Electrochem. Soc. 203 (2009) 119–124.
[35] B.P. Rai, Solar Cells 25 (1988) 265–272.